Supporting Information

Electrochemical Upcycling Biomass-Derived Methyl 2-Furoate and CO_2 into Monomers for Recyclable Polyesters

Pengfei Shi,[a,b] Xinyu Chai,[c] Yuefeng Wang,[b] Chenbao Lu,[*b] Huiping Ji,[*d] Yuezeng Su,[*a] and Xiaodong Zhuang[*b]

[a.] *School of Electronic Information and Electrical Engineering, Shanghai Jiao Tong University, Shanghai, P. R. China*

[b.] *The Soft2D Lab, State Key Laboratory of Synergistic Chem-Bio Synthesis, State Key Laboratory of Metal Matrix Composites, Shanghai Key Laboratory of Electrical Insulation and Thermal Ageing, School of Chemistry and Chemical Engineering, Shanghai Jiao Tong University, Shanghai 200240, China*

[c.] *School of Environmental Science and Engineering, Shanghai Jiao Tong University, Shanghai 201306, China.*

[d.] *Key Laboratory of Biomass Chemical Engineering of Ministry of Education, College of Chemical and Biological Engineering, Zhejiang University, Hangzhou, China Institute of Zhejiang University-Quzhou, Quzhou, China*

1. General Information

1.1 Materials and Reagents

Methyl 2-furoate, ethylene glycol, isosorbide, methanol, titanium(IV) isopropoxide ($Ti(OiPr)_4$), toluene, and zinc acetate ($Zn(OAc)_2$), were purchased from Adamas, Sigma-Aldrich, and TCl. They were used as received without further purification. Anhydrous solvents (Dichloromethane (DCM), N,N-Dimethylformamide (DMF), N-Methyl-2-Pyrrolidone (NMP), and Dimethyl Sulfoxide (DMSO)) were purchased from Adamas and used without further purification. Deuterated solvents (Methanol-D_4 and Chloroform-D) were purchased from Adamas. The supporting electrolytes—tetrabutylammonium iodide ($^nBu_4NI$), tetrabutylammonium bromide ($^nBu_4NBr$), tetrabutylammonium tetrafluoroborate ($^nBu_4NBF_4$), tetrabutylammonium hexafluorophosphate ($^nBu_4NPF_6$), and tetrabutylammonium perchlorate ($^nBu_4NClO_4$)—were purchased from Adamas. Prior to use, they were recrystallized from ethanol and dried under vacuum (at 80 °C for 24 hours for all salts, except for tetrabutylammonium perchlorate, which was dried at 40 °C for 48 hours).

1.2 Characterization

Liquid nuclear magnetic resonance (NMR) spectra were recorded on a Brucker AVANCE III HD 500 (500 MHz) spectrometer with tetramethylsilane as internal reference. Thermal gravimetric analysis (TGA) was performed on a Discovery TGA550 thermogravimetric analyzer to investigate the thermal stability of all samples in nitrogen atmosphere from ambient temperature to 550 °C at 10 °C min^{-1}. Differential Scanning Calorimetry (DSC) measurements were conducted on a Perkin Elmer Diamond series DSC. The temperature range used was ambient temperature up to 300 °C at a heating rate and cooling rate of 10 °C min^{-1}. Gel permeation chromatography (GPC) was performed on a Shimadzu LC-20AD XR system equipped with both UV and refractive index (RI) detectors. The system was calibrated with narrow dispersity polystyrene standards. Gas chromatography-mass spectrometry (GC-MS) analysis was performed on a Thermo Fisher Scientific ISQ7000 system equipped with an EI ion source. X-ray diffraction (XRD) patterns were performed on a RigakuD/Max 2500 X–ray diffractometer with Cu Karadiation (k=1.54 Å) at age neater voltage of 40 kV and a generator current of 40 mA.

2. General procedure of electrochemical C–H carboxylation.

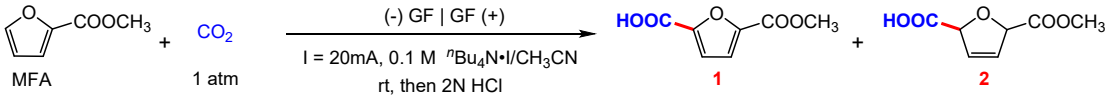

Electrochemical synthesis was performed using a reactor (Model LH-618-C) from the LH Labware company. All reaction vials and stir bars were dried in an oven at 120 °C for 3–4 hours and stored under vacuum in a desiccator until use. All electrodes, including graphite felt (GF), platinum (Pt), magnesium (Mg), and zinc (Zn), were purchased from LH Labware. Prior to use, the Mg and Zn electrodes were mechanically polished with 360-grit sandpaper. The electrocatalytic reaction was conducted in an undivided cell (20 mL) equipped with a magnetic stir bar and graphite felt (GF; 10 × 15 × 5 mm) electrodes. The cell was charged with MFA (0.8 mmol, 1.0 equiv.) and $^{n}Bu_4NI$ (295.5 mg, 0.8 mmol, 1.0 equiv.) under a CO_2 atmosphere. The system was evacuated and back-filled with CO_2 (three cycles), after which anhydrous CH_3CN (8.0 mL) was added via syringe. Electrocatalysis proceeded at a constant current of 20.0 mA for 3.5 h under a CO_2 balloon. Upon completion, the reaction mixture was acidified with aqueous HCl (2.0 M). The mixture was extracted with EtOAc (5 × 15 mL), and the combined organic layers were washed with saturated NH_4Cl solution, dried over anhydrous $MgSO_4$, filtered, and concentrated under reduced pressure. The crude yield and ratio were determined by GC-MS analysis of the resulting material. The crude product was purified by column chromatography using MeOH/EtOAc (1:5, v/v) containing 1% acetic acid as the eluent to afford the desired product.

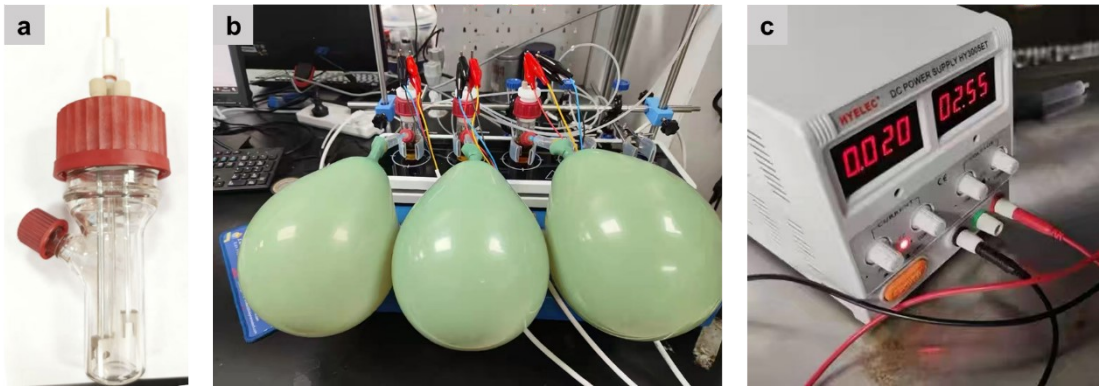

Fig. S1 (a) Experimental setup and tools. (b) General reaction apparatus. (c) Potentiostat for electrolysis.

3. Characterization of Products

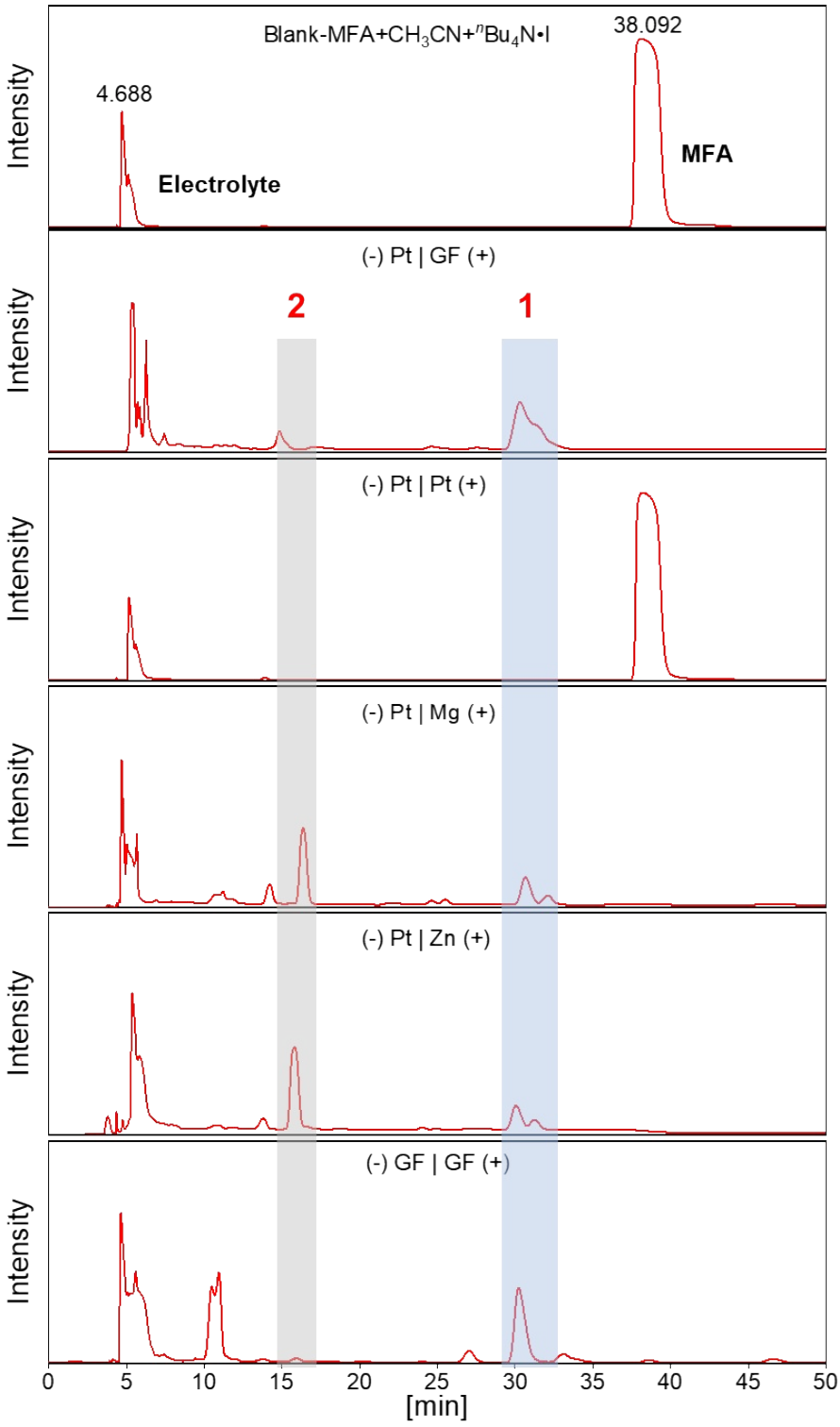

Fig. S2 GC-MS chromatograms of reaction mixtures under different electrode combinations, highlighting the peak locations of the starting material (MFA), electrolyte, and Products 1 and 2. A slight overall shift in retention time is attributed to instrumental drift.

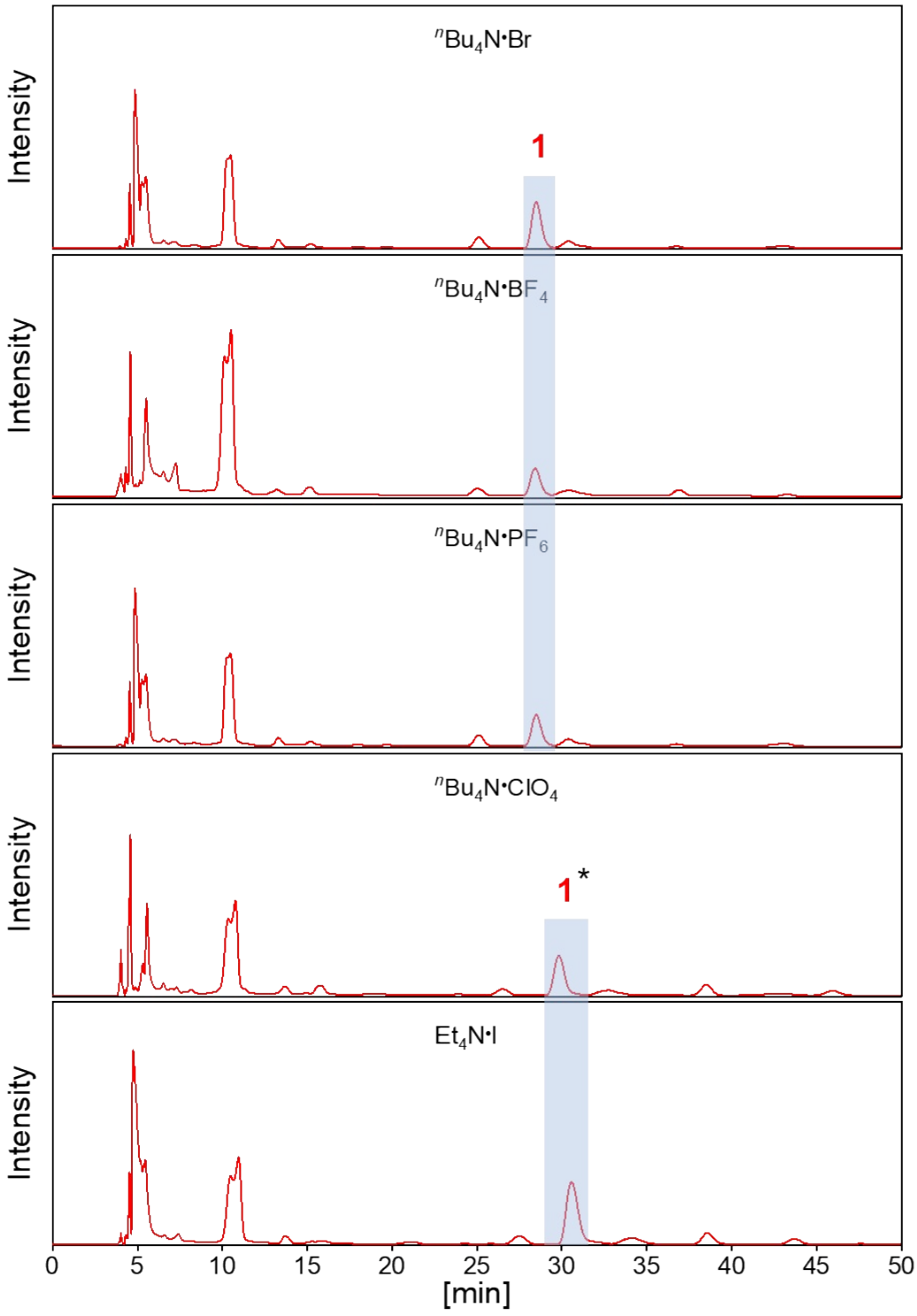

Fig. S3 GC-MS chromatograms of reaction mixtures with different electrolytes, highlighting the peak corresponding to Product 1. * A slight overall shift in retention time (e.g., at around 11, 27.5, 30.5, and 34 min) is attributed to instrumental drift; GC–MS spectra confirm that the same compound 1 was detected in all experiments.

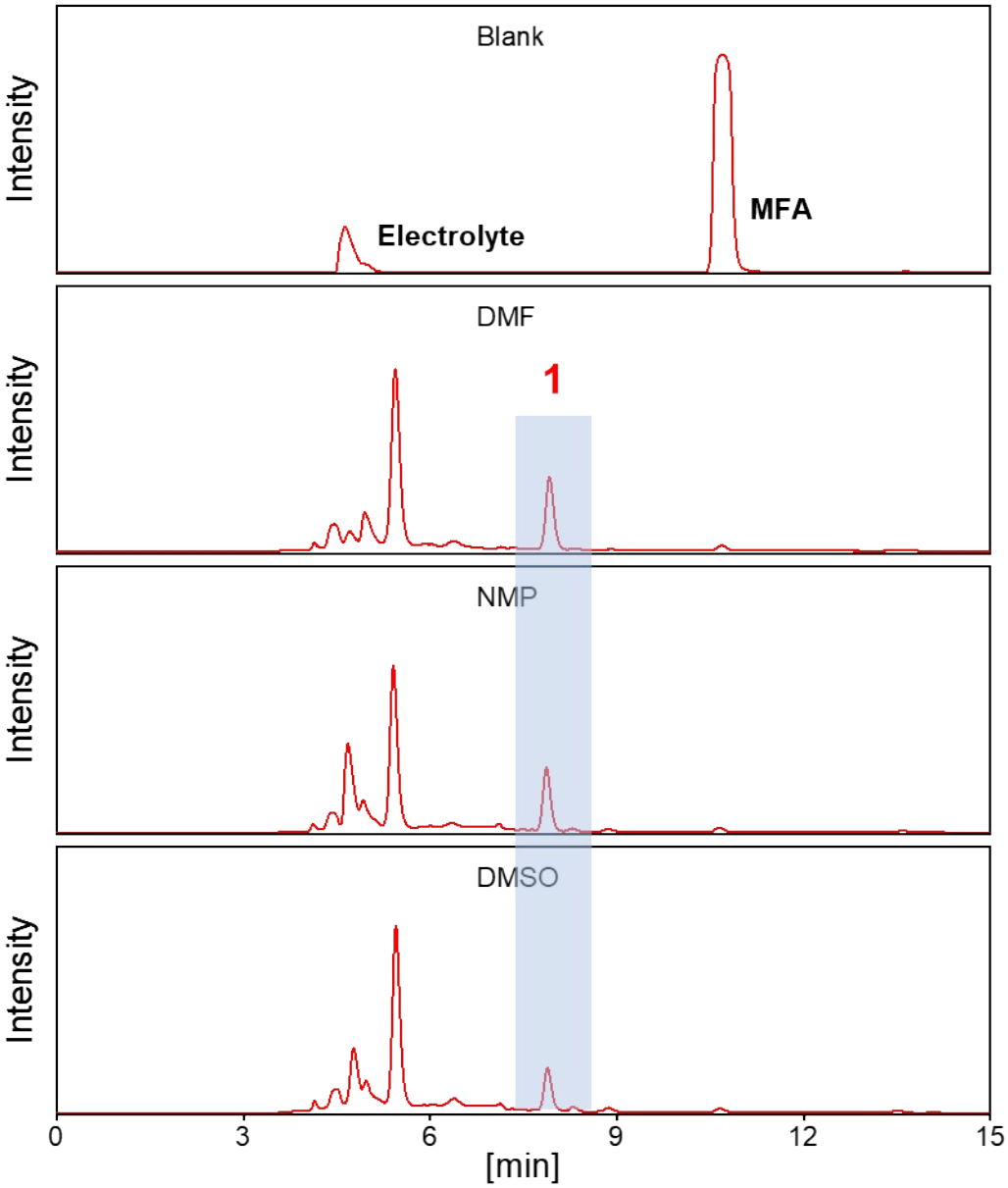

Fig. S4 GC-MS chromatograms of reaction mixtures with different solvents, highlighting the peak corresponding to Product 1. Retention time difference compared with Figures S2–S3 results from the use of a different GC–MS instrument.

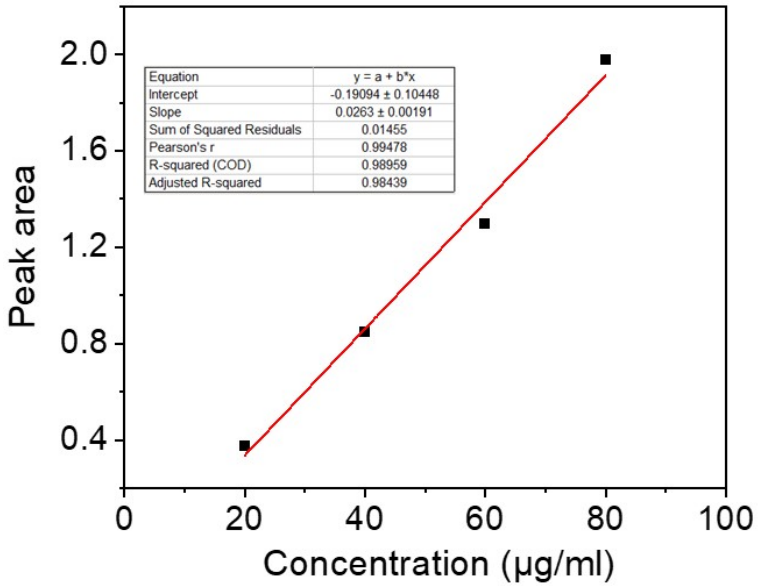

Fig. S5 Calibration curve for the quantitative analysis by GC-MS. The curve plots the analyte concentration against the peak area ratio, demonstrating a strong linear relationship with a correlation coefficient (R^2) of 0.9896.

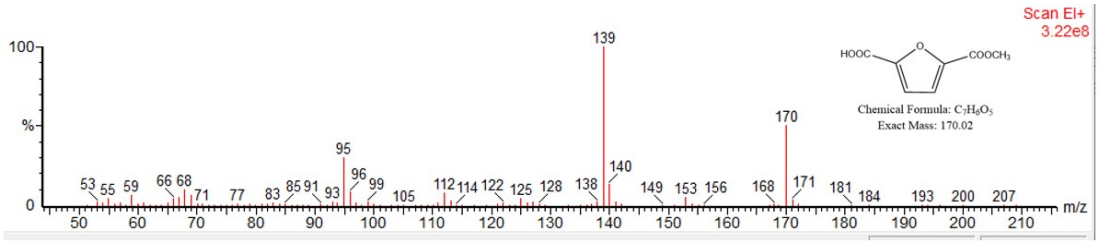

Fig. S6 EI mass spectrum of Product 1 acquired by GC-MS. MS (EI): m/z calcd. for $C_7H_6O_5$ $[M]^+$: 170.02, found 170.

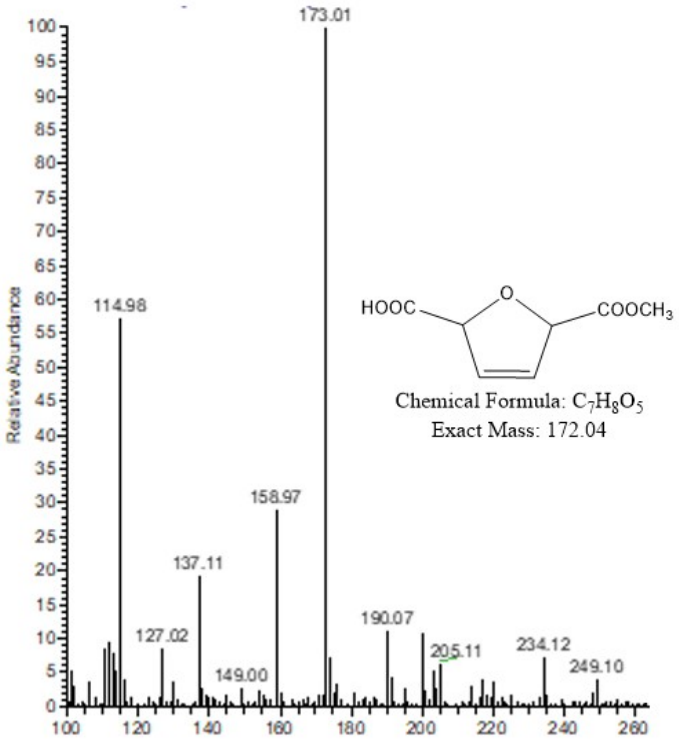

Fig. S7 CI mass spectrum of Product 2 acquired by GC-MS. HRMS (CI): m/z calcd. for $C_7H_8O_5$ $[M+H]^+$: 173.04, found 173.01.

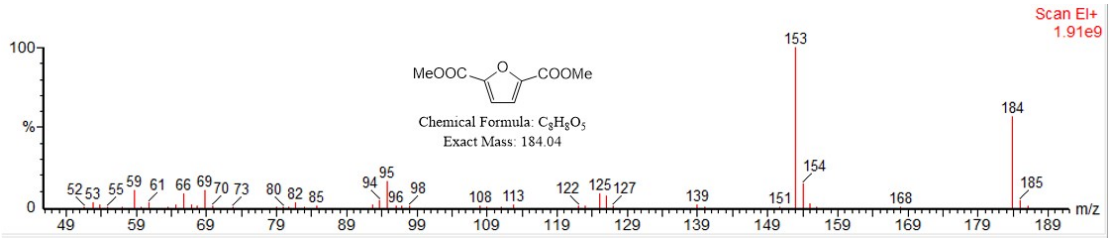

Fig. S8 EI mass spectrum of dm-FDCA acquired by GC-MS. MS (EI): m/z calcd. for $C_8H_8O_5$ $[M]^+$: 184.04, found 184.

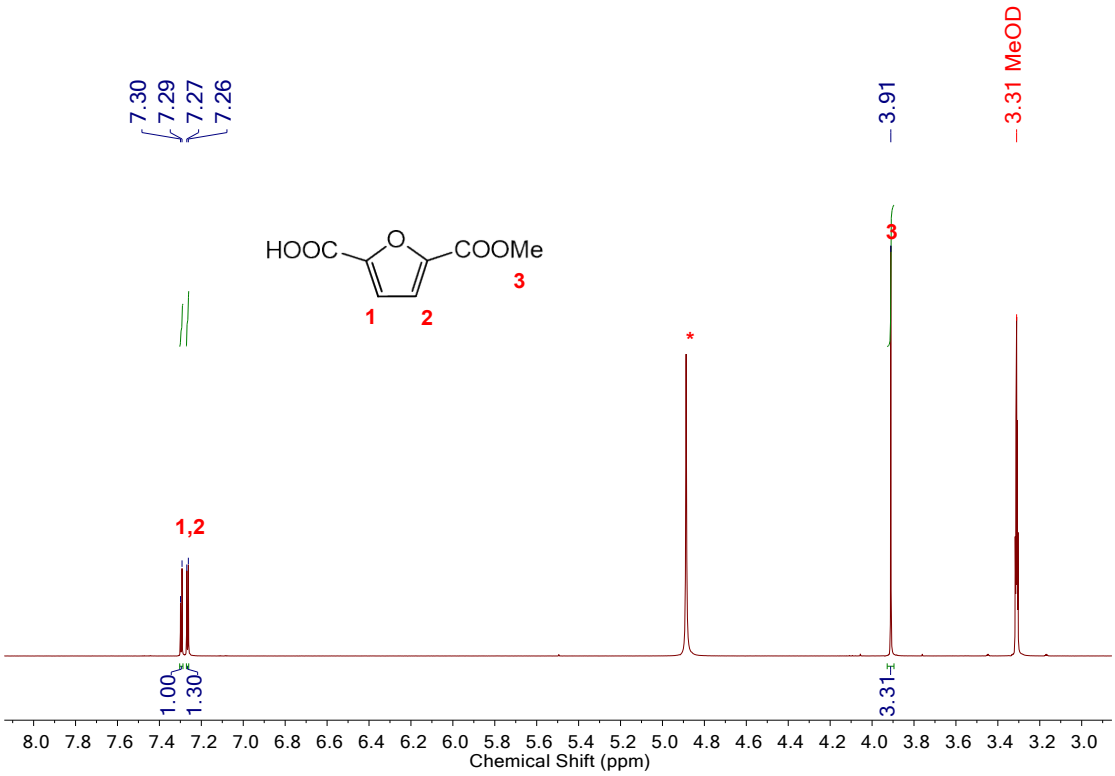

Fig. S9 ^{1}H NMR spectrum of Product 1 in Methanol-d$_4$. ^{1}H NMR (500 MHz, Methanol-*d*$_4$) δ = 7.30 (d, J = 3.6 Hz, 1H), 7.27 (d, J = 3.7 Hz, 1H), 3.91 (s, 3H). The asterisk (*) denotes a residual impurity peak. The analytical data corresponds with those reported in the literature.[4]

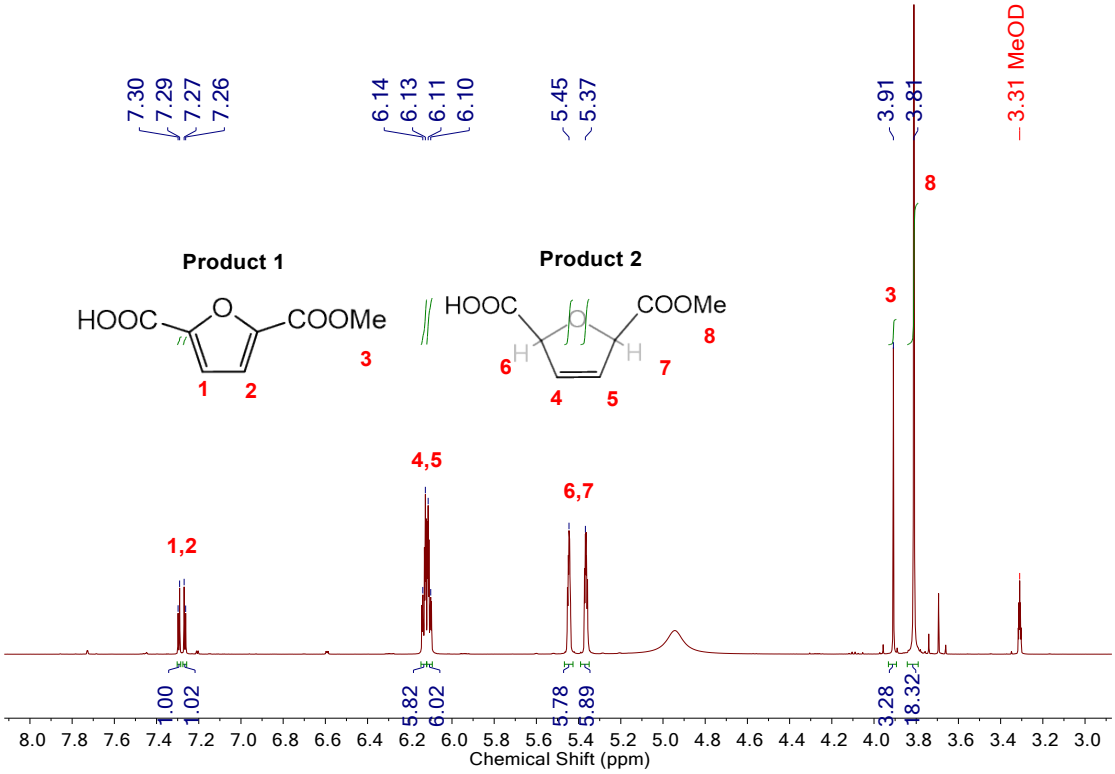

Fig. S10 ^{1}H NMR spectrum of the mixture of Product 1 and Product 2 in Methanol-d_4. **Product 1:** ^{1}H NMR (500 MHz, Methanol-d_4) δ = 7.30 (d, J = 3.6 Hz, 1H), 7.27 (d, J = 3.7 Hz, 1H), 3.91 (s, 3H). **Product 2:** ^{1}H NMR (500 MHz, Methanol-d_4) δ = 6.13 (d, J = 6.1 Hz, 1H), 6.11 (d, J = 6.1 Hz, 1H), 5.45 (s, 1H), 5.37 (s, 1H), 3.81 (s, 3H).

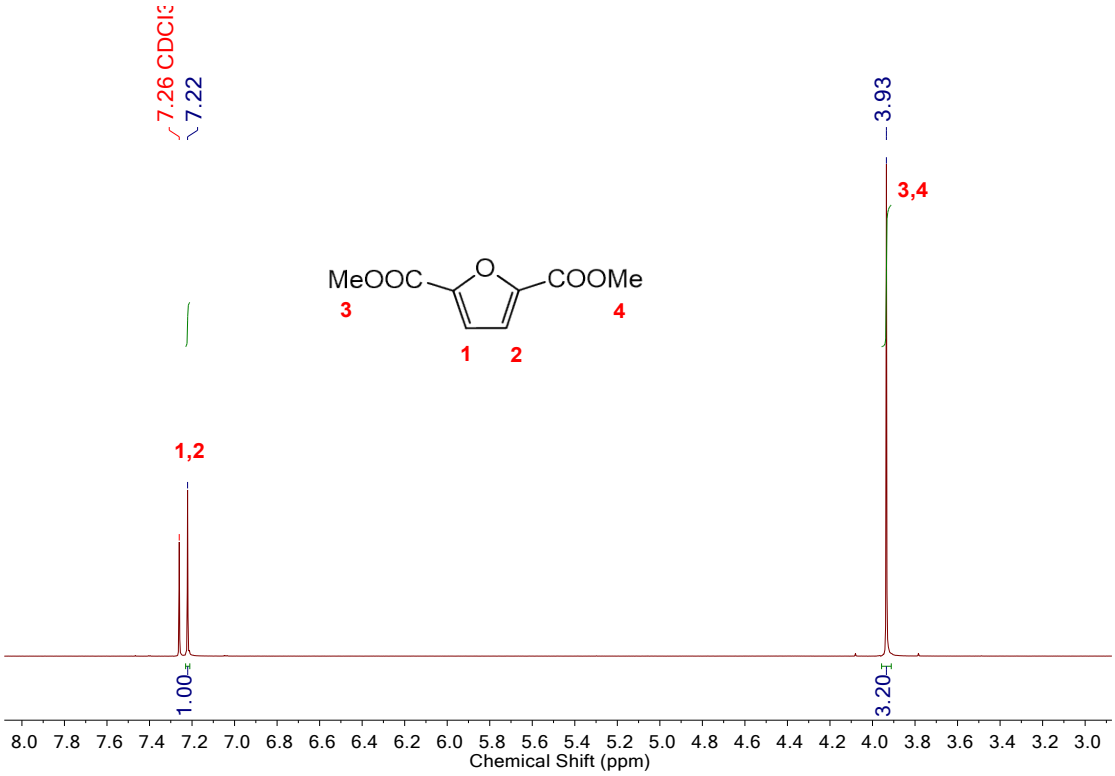

Fig. S11 ^{1}H NMR spectrum of the ester of Product 1 (dm-FDCA) in Chloroform-d. ^{1}H NMR (500 MHz, Chloroform-d) δ = 7.22 (s, 2H), 3.93 (s, 6H).

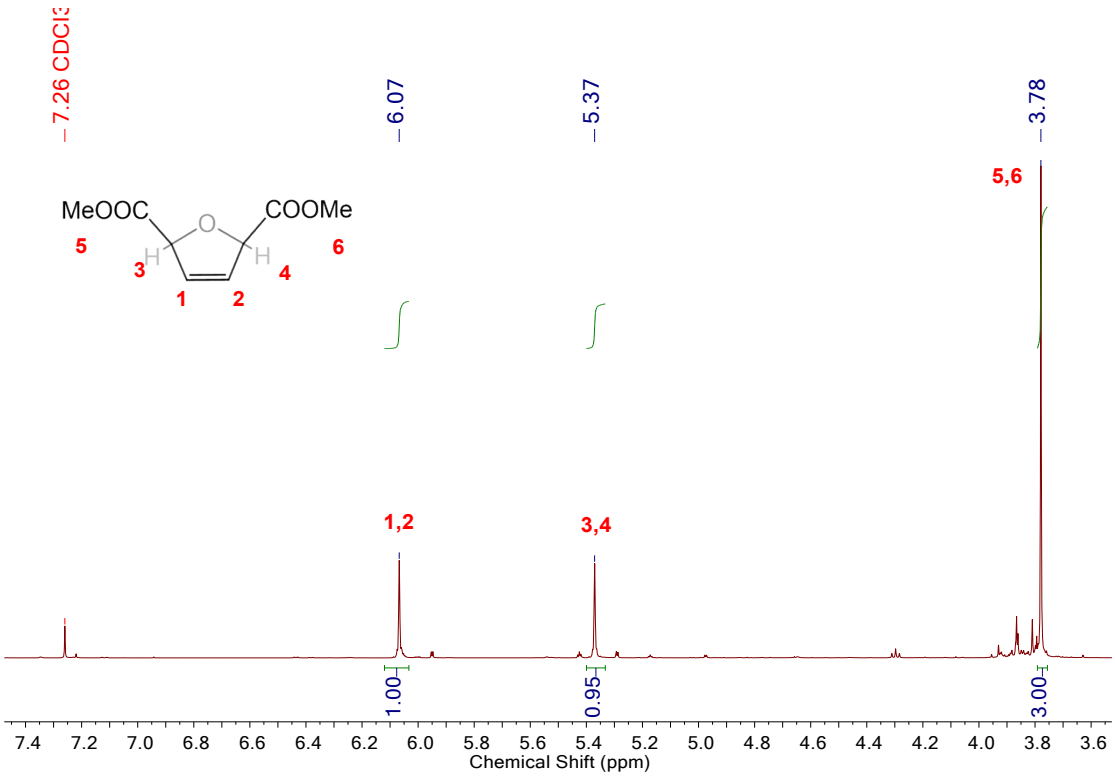

Fig. S12 ^{1}H NMR spectrum of the ester of Product 2 in Chloroform-d. ^{1}H NMR (500 MHz, Chloroform-d) δ = 6.07 (s, 2H), 5.37 (s, 2H), 3.78 (s, 6H). The analytical data corresponds with those reported in the literature.[5]

4. Details for Quantum Chemical Calculations

4.1 Computational Methods

All density functional theory (DFT) calculations were performed using the Gaussian 16 program. Geometry optimizations for the neutral (N electron) and anionic (N+1 electron) systems were carried out at the (U)B3LYP/6-31+G* level of theory. To evaluate the regioselectivity of nucleophilic attack, condensed Fukui functions for nucleophilic attack (f_A^+) were computed using Hirshfeld population analysis. The Hirshfeld charges for the neutral (q_N^A) and anionic (q_{N+1}^A) systems were obtained from single-point calculations on the optimized geometries, and the Fukui function values were determined as $f_A^+ = q_N^A - q_{N+1}^A$. Atomic charge distributions were calculated using Multiwfn 3.8 software.[6, 7] Electrostatic potential (ESP) surfaces were generated from quantum mechanical calculations and mapped onto molecular van der Waals surfaces using VMD. The reduction potentials were also calculated. The geometries of the neutral molecules and their corresponding radical anions were optimized at the (U)B3LYP/6-31+G(d,p) level, with solvation effects accounted for by the CPCM model with acetonitrile (CH_3CN) as the solvent. The Gibbs free energy change for the one-electron reduction was calculated as $\Delta G_{1/2} = G_{298}[radical\ anion] - G_{298}[neutral]$. The half-wave reduction potential ($E_{1/2}^{cal.}$) versus the saturated calomel electrode (SCE) in acetonitrile was computed using the equation:

$$E_{1/2}^{cal.} = -\Delta G_{1/2}/n_e F - E_{1/2}^{SHE}(4.281) + E_{1/2}^{SCE}(-0.141)$$

where $\Delta G_{1/2} = G_{298}[radical\ anion] - G_{298}[neutral]$, n_e = 1, and F = 23.061 kcal·mol^{-1}·V^{-1}.

4.2 Computed Cartesian Coordinates for Optimized Geometries (Å)

CO_2

Charge = 0 Spin Multiplicity = 1

C	-0.25506500	0.10770700	-3.25124800
O	-0.38024500	-0.95379700	-3.81191400
O	-0.12999000	1.16889000	-2.69033900

$CO_2^{\bullet-}$

Charge = -1 Spin Multiplicity = 2

C	-0.18244900	0.24503600	-3.52744200
O	-0.41048900	-0.97105000	-3.64666700
O	-0.17236100	1.04881400	-2.57939200

MFA

Charge = 0 Spin Multiplicity = 1

C	-0.07700900	-2.38666300	0.12864900
C	0.06803600	-1.21388600	0.81876500
C	-0.01393700	-0.17114400	-0.15170600
C	-0.20340400	-0.78401400	-1.36509200
O	-0.24281000	-2.14476900	-1.19764400
C	-0.36306300	-0.28629100	-2.72920100
O	-0.52943400	-0.99139200	-3.71464900
O	-0.30318500	1.05776600	-2.76379200
C	-0.44782800	1.66946500	-4.06432500
H	-0.08461800	-3.42457000	0.42313000

H	0.21453300	-1.10996000	1.88374700
H	0.05658500	0.89306200	0.01616000
H	0.34792300	1.33094700	-4.73070700
H	-0.37007800	2.74034400	-3.88657600
H	-1.42070900	1.42000500	-4.49226000

MFA$^{\bullet-}$

Charge = -1 Spin Multiplicity = 2

C	-0.04573300	-2.40403500	0.15029500
C	0.10453300	-1.20528300	0.80597800
C	-0.02088000	-0.16729800	-0.15179800
C	-0.24898700	-0.79110900	-1.40314200
O	-0.26648200	-2.18346100	-1.20367000
C	-0.46099300	-0.31698000	-2.70627000
O	-0.64334000	-0.99346500	-3.76490000
O	-0.48288600	1.09290400	-2.74337400
C	-0.41662500	1.67322400	-4.04294500
H	-0.02740000	-3.43597300	0.46339500
H	0.28664600	-1.09023100	1.86719700
H	0.04641200	0.89689600	0.01770400
H	0.51439900	1.40255400	-4.55591100
H	-0.44634900	2.75410000	-3.89023300
H	-1.26131500	1.36705700	-4.66782500

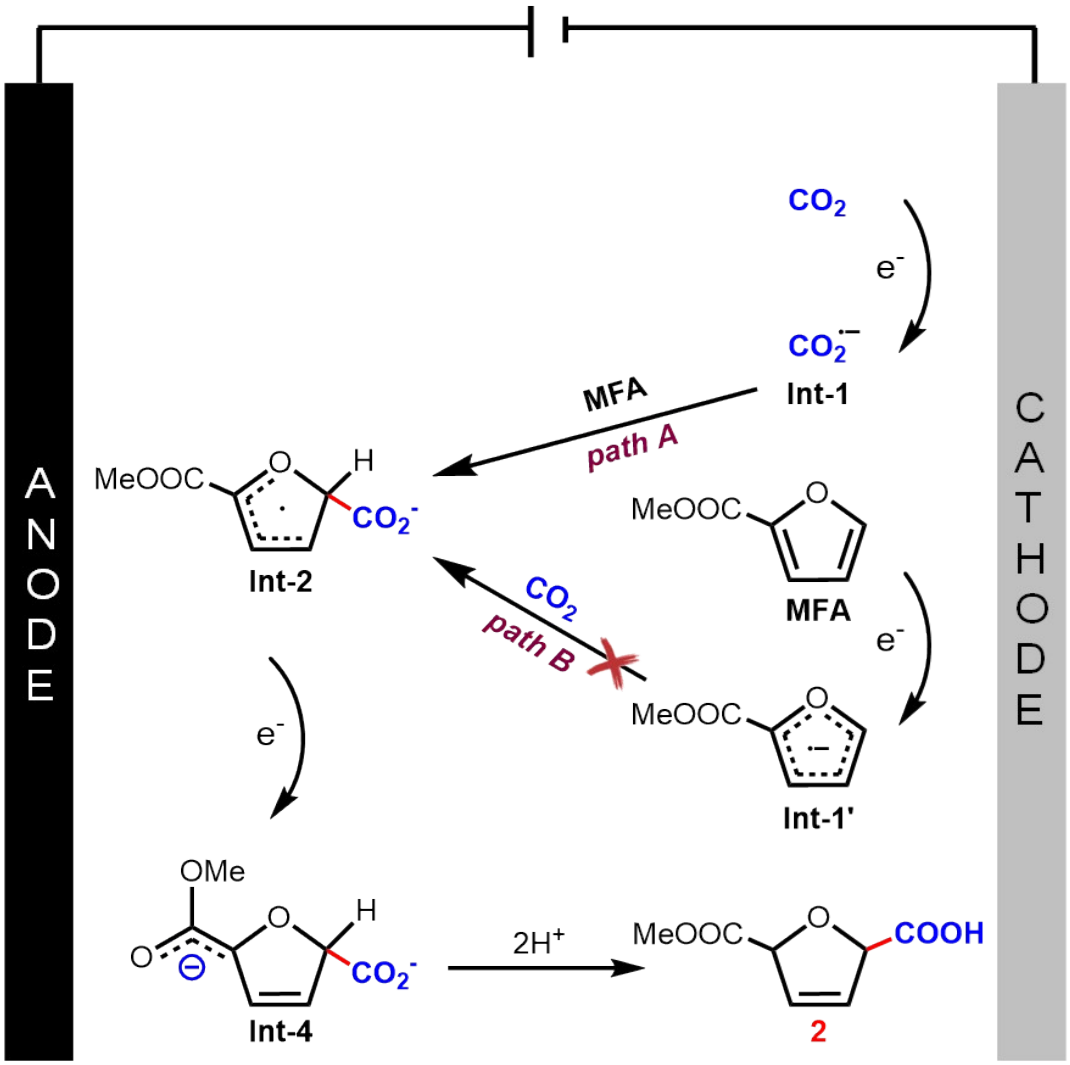

Fig. S13 A plausible mechanism of product 2.

5. Gram-scale Experiment

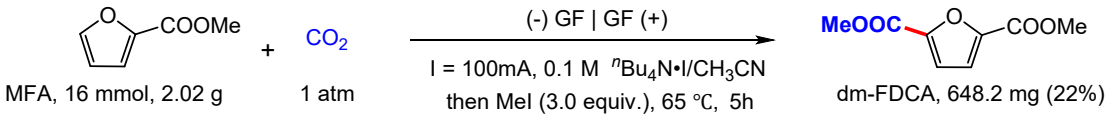

The electrocatalytic reaction was conducted in a 500 mL three-neck flask equipped with a magnetic stir bar and graphite felt (GF, 30 × 45 × 5 mm) electrodes. The two side necks of the flask were fitted with copper wires, which served as electrical leads connected to the graphite felt electrodes. The cell was charged with MFA (2.02 g, 16 mmol, 1.0 equiv.) and $^nBu_4NI$ (5.91 g, 16 mmol, 1.0 equiv.) under a CO_2 atmosphere. The system was evacuated and back-filled with CO_2 (three cycles), after which anhydrous CH_3CN (160 mL) was added via syringe. Electrocatalysis proceeded at a constant current of 100 mA for 12 h under a CO_2 balloon. Following the completion of electrolysis, iodomethane (3.0 mL, 3.0 equiv) was added to the reaction mixture via syringe under a nitrogen atmosphere. The resulting mixture was stirred at 65 °C for 5 h to complete the methylation. After cooling to room temperature, the mixture was extracted with EtOAc (5 × 80 mL). The combined organic extracts were washed with saturated NH_4Cl solution, dried over anhydrous $MgSO_4$, filtered, and concentrated under reduced pressure. Purification of the residue by column chromatography using EtOAc/PE (3:7, v/v) as the eluent afforded dm-FDCA (648.2 mg, 22%).

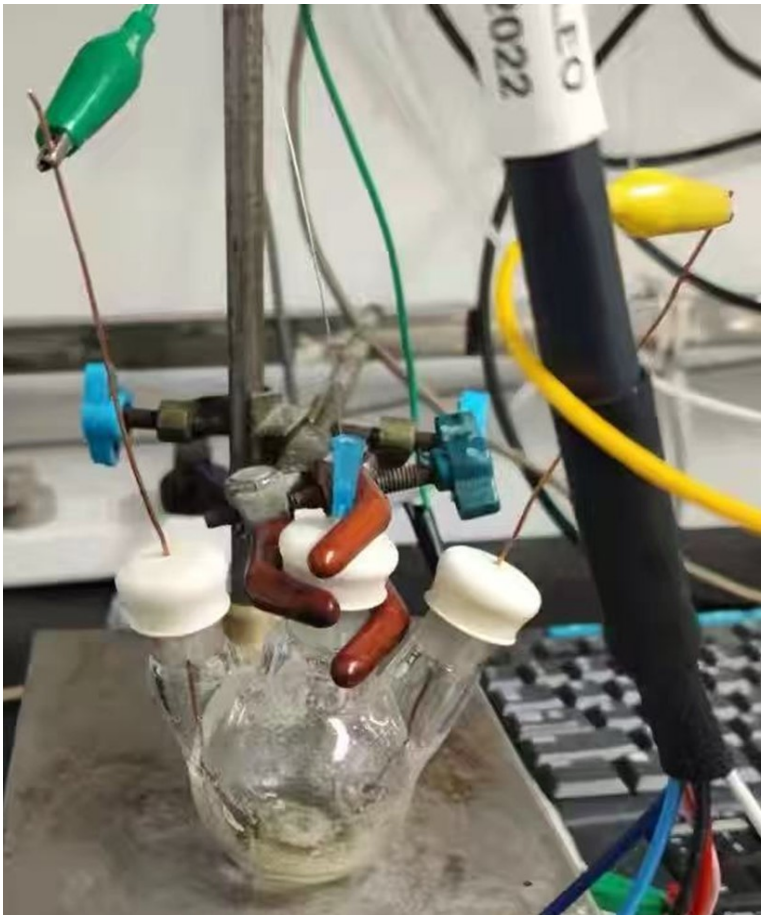

Fig. S14 Photograph of the gram-scale synthesis apparatus.

6. Polymerization

In a typical experiment, the polycondensation reaction was carried out in a 100 mL three-necked round-bottom flask equipped with nitrogen circulation system and water condenser. dm-FDCA (8 mmol) and diols (16 mmol) were charged into the reaction flask. The system was evacuated and purged with nitrogen, and this cycle was repeated three times. The polycondensation procedure consisted of two stages. In the first stage, the reaction was conducted under nitrogen atmosphere to form oligomers. The reaction mixture was preheated at 115 °C in a silicone oil bath with continuous stirring for 15 minutes, after which the catalyst $Ti(OiPr)_4$ (1.25 mol%) dissolved in 1 mL of toluene was added to the flask under a continuous nitrogen flow. The temperature was then raised to 170–180 °C and maintained for 2.5 hours with stirring, during which methanol and toluene were collected in a cooled receiving flask to complete the first stage of prepolymerization. In the second stage of polycondensation, the temperature was increased to 230–240 °C. To obtain high molecular weight polyester, a high vacuum of 0.02 mbar was gradually applied and maintained for 3 hours. Upon completion of the reaction, the mixture was cooled to room temperature under nitrogen. The polymer was dissolved and precipitated in 100 mL of methanol, filtered, and vacuum-dried at 60 °C for 12 hours to yield a white powder.

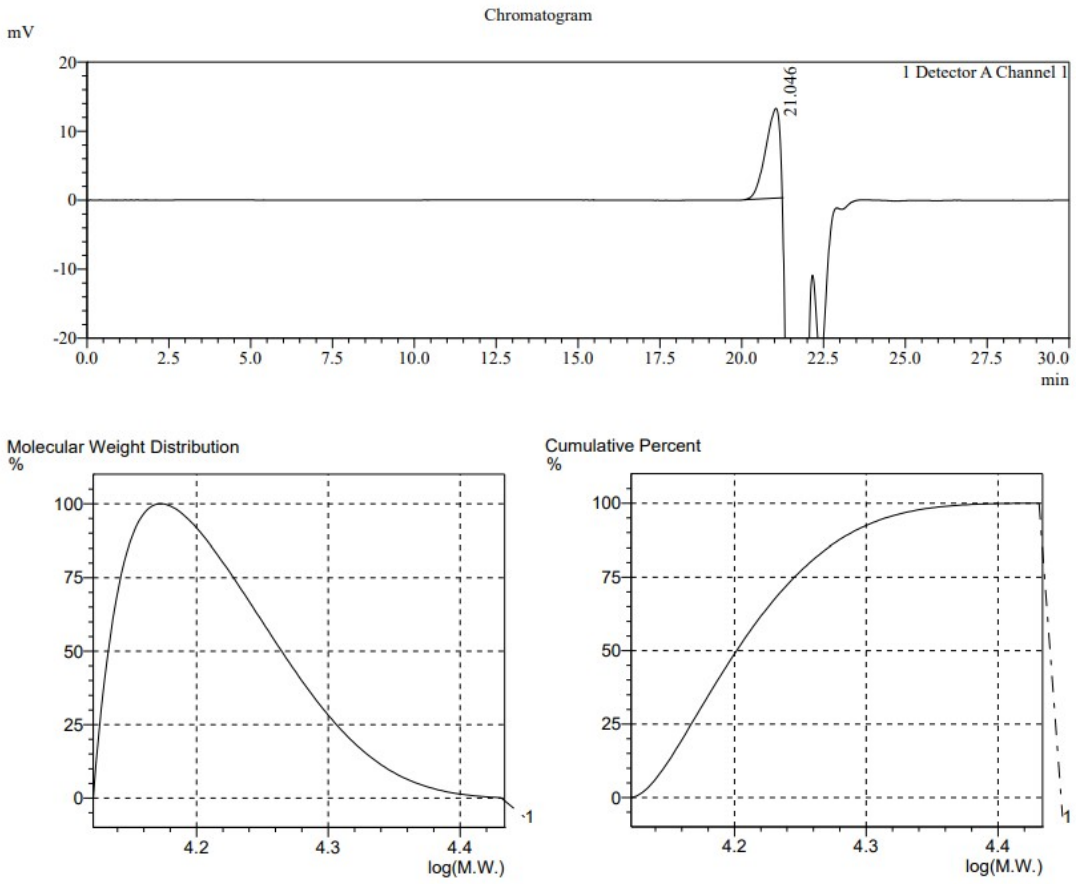

Fig. S15 GPC chromatogram (top) and molecular weight distribution curves (bottom) of the PEF.

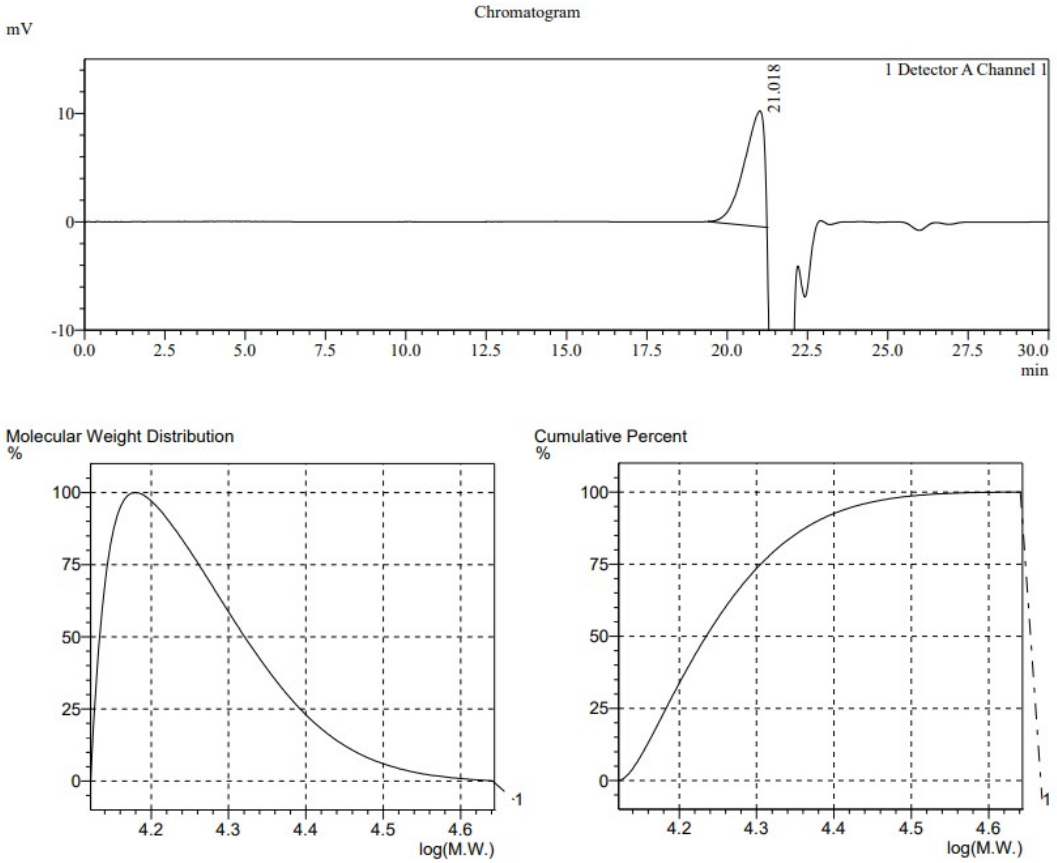

Fig. S16 GPC chromatogram (top) and molecular weight distribution curves (bottom) of the PIF.

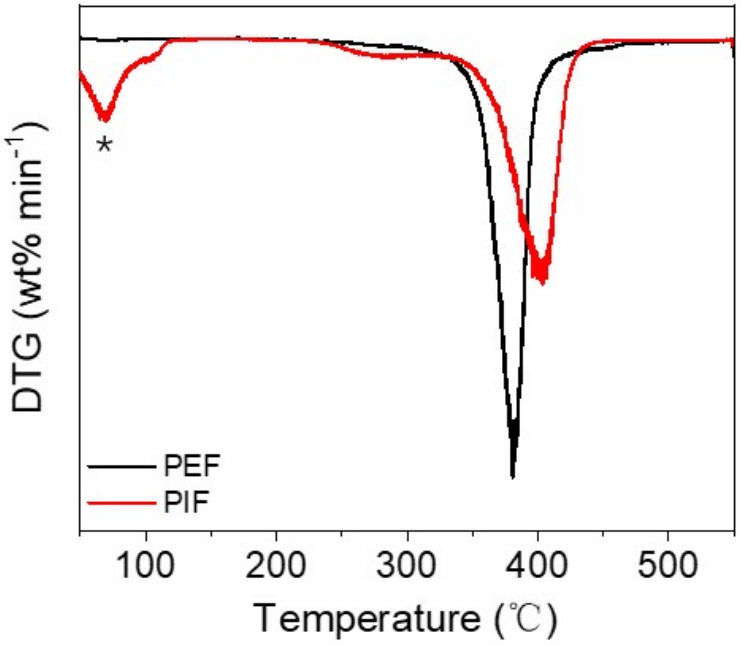

Fig. S17 Derivative thermogravimetry (DTG) curves of PEF and PIF. Note: the significant mass loss below 150 °C of PIF (*) is attributed to the evaporation of residual solvent.

7. Depolymerization

The depolymerization of PEF and PIF was performed following a methanolysis protocol.[8] In a typical experiment, the polyester (1.0 mmol, based on the monomer unit) was placed in a sealed reaction vessel, followed by the addition of methanol (70 equiv., 70 mmol) as the depolymerization reagent. $Zn(OAc)_2$ was added as the catalyst (1.0 mol% relative to the monomer unit), and the mixture was heated at 120 °C for 5 h. After completion, methanol was removed under reduced pressure. A defined amount of the resulting residue was dissolved in 1.0 mL of dichloromethane, filtered through a PTFE syringe filter, and directly analyzed by GC–MS. Quantification of dm-FDCA was performed using an external calibration curve. The total amount of dm-FDCA produced in the reaction is calculated:

$$n_{prod,total} = \frac{(\frac{A_{sample} - b}{m})V_{sol}}{M_{dm-FDCA}} \times \frac{M_{residue}}{m_{aliquot}}$$

Here, A_{sample} is the GC–MS peak area of dm-FDCA in the analyzed aliquot, m and b are the slope and intercept of the external calibration curve, V_{sol} is the solution volume used for GC–MS analysis, $M_{\text{dm - FDCA}}$ is the molar mass of dm-FDCA, m_{aliquot} is the mass of the aliquot taken, and M_{residue} is the total mass of the reaction residue.

The overall depolymerization yield relative to the theoretical monomer content is then determined using:

$$Yield(\%) = \frac{n_{prod,total}}{m_{polymer}/M_{monomer}} \times 100\%$$

where m_{polymer} is the mass of the starting polyester and M_{monomer} is the molar mass of the corresponding monomer unit.

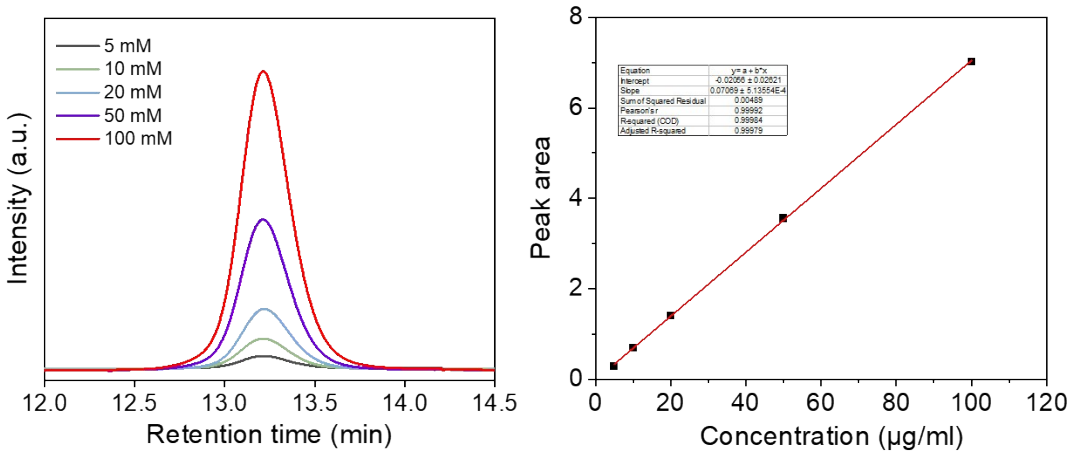

Fig. S18 (a) GC–MS chromatograms of dm-FDCA standard solutions at different concentrations. (b) Calibration curve constructed using GC–MS peak area versus concentration, fitted with a linear regression model. The correlation coefficient (R^2 = 0.99979) confirms excellent linearity over the tested concentration range.

Table S1. Computed Hirshfeld charges for the neutral (q_N^A) and anionic (q_{N+1}^A) states, and the resulting condensed Fukui function values for nucleophilic attack (f_A^+) at the key positions of MFA.

Position	q_N^A	q_{N+1}^A	f_A^+
C3	-0.05987035	-0.15989839	0.100
C4	-0.07885675	-0.13728349	0.058
C5	0.03392283	-0.07693674	0.111

Table S2. Calculated Gibbs free energies and reduction potentials for MFA and CO_2.

Compound	$G_{298}[neutral]$ (Hartree)	$G_{298}[radical\ anion]$ (Hartree)	$\Delta G_{1/2}$ (kcal/mol)	$E_{1/2}^{cal.}$ (V vs. SHE)
MFA	-457.9596	-458.0349	-47.2	-2.37
CO_2	-188.58964	-188.67957	-56.4	-1.98

Table S3. Results of the polymerization between dm-FDCA and various diols.

Polymer	M_n (g mol^{-1})	M_w (g mol^{-1})	PDI	Yield (%)	Appearance
PEF	16159	16421	1.01	76	Translucent
PIF	17599	18361	1.04	69	Translucent

Table S4. Summary of thermal characteristics for PEF and PIF derived from TGA and DSC analyses. The data include the temperatures at 5% mass loss ($T_{d,5\%}$) and maximum decomposition rate ($T_{d,max}$) from TGA, as well as glass transition temperature (Tg), cold-crystallization temperature and enthalpy (Tc, ΔHc), and melting temperature and enthalpy (Tm, ΔHm) from DSC.

Polymer	$T_{d,5\%}$ (℃)	$T_{d,max}$ (℃)	Tg (℃)	Tc (℃)	Tm (℃)	ΔHc (J g^{-1})	ΔHm (J g^{-1})
PEF	324	381	78	164	214	-10.5	17.8
PIF	285	404	90	193	288	-1.6	0.7

Table S5. Comparison of different synthetic routes toward FDCA and its derivatives.

Route	Reaction conditions	Energy input	Process complexity	Yield	Environmental friendliness	Carbon utilization	Scalability / Safety	Reference
(1) Disproportionation of 2-furoic acid	160–200 °C; homogeneous catalyst	moderate heating	single step	65%	moderate waste	no CO_2 fixation	thermal operation	ChemSusChem, 2013, 6
(2) Four-step carbonylation route	bromination, esterification, Pd-catalyzed carbonylation, hydrolysis; multi-step	high energy	four steps	65%	halogens; multiple organic solvents	no CO_2 fixation	complex process; safety issues	ACS Sustain. Chem. Eng, 2018, 6, 13192-13198
(3) Cs_2CO_3-promoted C–H carboxylation	150–200 °C; molten Cs_2CO_3; high pressure	high energy	single step	89%	low waste	direct CO_2 fixation	high temperature and pressure operation; safety issues	Nature, 2016, 531, 215-219
(4) Electrochemical C–H carboxylation	ambient temperature; catalyst-/base-free	electricity only	single step	27%	low waste	direct CO_2 fixation	ambient; safe; scalable	***this work***

References

1. R. A. Sheldon, *ACS Sustainable Chemistry & Engineering*, 2018, **6**, 32-48.
2. R. Chauvy, R. Lepore, P. Fortemps and G. De Weireld, *Sustainable production and Consumption*, 2020, **24**, 194-210.
3. Z. Wang, S. R. Nabavi and G. P. Rangaiah, *Processes*, 2024, **12**, 2532.
4. Y. Shen, B. Yao, G. Yu, Y. Fu, F. Liu and Z. Li, *Green Chemistry*, 2017, **19**, 4930-4938.
5. W. J. Gensler, S. Chan and D. B. Ball, *The Journal of Organic Chemistry*, 1981, **46**, 3407-3415.
6. D. Ju, Y. Park, M. Noh, M. Koo and S. Kim, *The Journal of Chemical Physics*, 2024, **161**.
7. T. Lu and F. Chen, *Journal of computational chemistry*, 2012, **33**, 580-592.
8. C. Alberti, K. Matthiesen, M. Wehrmeister, S. Bycinskij and S. Enthaler, *ChemistrySelect*, 2021, **6**, 7972-7975.